Multivariate Statistics of Disposition Pharmacokinetic Parameters for Structurally Unrelated Drugs Used in Therapeutics

Vangelis Karalis,[1] Anna Tsantili–Kakoulidou,[2] and Panos Macheras[1, 3]

Received May 20, 2002; accepted August 22, 2002

Purpose. To explore the quantitative structure pharmacokinetic relationships of the disposition parameters: clearance (CL), apparent volume of drug distribution (V_{ap}), fractal clearance (CL_f), and fractal volume (v_f) for 272 structurally unrelated drugs used in therapeutics.
Methods. Literature data were used for CL and V_{ap} whereas CL_f and v_f were estimated as described previously (*Pharm. Res*. 18, 1056, 2001 and 19, 697, 2002). A variety of molecular descriptors expressing lipophilicity, ionization, molecular size and hydrogen bonding capacity were estimated using computer packages. The data were analyzed using multivariate statistics. For each disposition parameter (CL, V_{ap}, CL_f, v_f) PCA (principal component analysis) and PLS (projection to latent structures) were applied to the total set of data as well as to subsets of data.
Results. Drugs were divided into two classes (I and II) according to their v_f/V_{ap} ratio. Class I comprises 131 drugs with $v_f/V_{ap}>1$, whereas class II 141 drugs with $v_f/V_{ap} < 1$. After initial PLS analysis, class I was subdivided in subclusters I_a (30 drugs) and I_b (101 drugs). It was found that I_a included mostly acidic drugs with high protein binding, whereas class II comprises mainly basic, lipophilic compounds. No correlation was found between CL, V_{ap}, CL_f and the used descriptors. Adequate PLS models were derived for v_f considering subclusters I_a, I_b and class II separately. The low v_f values of class I_a drugs were affected negatively from molecular size descriptors and non-polar surface area. For class I_b drugs with intermediate v_f values, apparent lipophilicity contributed positively, although molecular size descriptors and polarity were inhibitory factors. The high v_f values of class II drugs were positively dependent on intrinsic lipophilicity and increased basicity, whereas polarity entered with negative contribution.
Conclusions. The parameters V_{ap}, CL, and CL_f fail to reflect the physicochemical properties of drugs. The transformation of V_{ap} values to v_f is the underlying cause for the valid models for v_f. These models allow a global consideration of molecular properties (lipophilicity, ionization, molecular size, polar surface area) which govern the distribution of drugs in the human body. The present study provides additional evidence for the physiologically sound concept of v_f.

KEY WORDS: multivariate statistics; disposition parameters; fractal volume; apparent volume of distribution; fractal clearance; clearance.

INTRODUCTION

The development of quantitative structure pharmacokinetic relationships (QSPR) models focuses on the association of structural features of chemicals, either to their pharmacokinetic (PK) determinants (e.g., partition coefficient), solubility or to PK parameters (e.g., volume of distribution), half-life (1). The utility of the models relies on the fact that they can be further used to predict the PK properties of new chemical compounds. Several successful attempts have been reported to establish QSPR models utilizing a variety of PK parameters within congeneric series of drug molecules (2–12). However, there have been only limited efforts in establishing QSPR models for structurally unrelated drugs (13–17).

In the field of drug disposition, the quantitative relationships between structural features of drugs and their PK parameters are complicated by the composite nature of processes (i.e., both distribution and elimination processes are involved). When clearance, CL, is not derived from the quotient $Dose/AUC$, the fictitious numerical values of the apparent volume of distribution, V_{ap}, can affect the CL estimates, and make their use questionable in QSPR modeling for structurally unrelated compounds. However, a more physiologically relevant description of drug distribution and elimination was published recently (18,19). The new parameters used to describe distribution and elimination, fractal volume of distribution, v_f, and fractal clearance, CL_f, respectively were found to exhibit better behavior than the conventional parameters V_{ap} and CL in interspecies PK scaling (18,19). These observations prompted us to explore in a comparative manner the relationships between each one of the disposition parameters, V_{ap}, CL, v_f, and CL_f and relevant molecular descriptors. To this end, a large number of structurally unrelated drugs, currently used in therapeutics (20), was analyzed. Due to the diversity and the complexity of the data, the whole task was performed using multivariate data analysis (MVDA). MVDA is a powerful statistical tool, widely used, based on the projection method to extract latent variables from a large set of descriptors, thus reducing a complicated multidimensional space to a small number of components. It permits the use of interrelated descriptors, can handle multiple responses in the same model, and is useful to detect outliers and to categorize data in different classes (21–24).

METHODS

The drugs used for analysis were obtained from a classic textbook of pharmacology (20). A total of 314 drugs were found to be accompanied with the PK parameters under study

[1] Laboratory of Biopharmaceutics-Pharmacokinetics, School of Pharmacy, University of Athens, Athens, Greece.
[2] Laboratory of Pharmaceutical Chemistry, School of Pharmacy, University of Athens, Athens, Greece.
[3] To whom correspondence should be addressed. (e-mail: macheras@pharm.uoa.gr).

ABBREVIATIONS: PK, Pharmacokinetics; QSPR, Quantitative Structure Pharmacokinetic Relationships; MVDA, Multivariate Data Analysis; PCA, Principal Component Analysis; PLS, Projection to Latent Structures; *CV,* Cross Validation; RMSEP, Root Mean Square Error of Prediction; t_1, The coordinates of the principal component extracted from the **X** matrix after PLS; u_1, The coordinates of the PK parameter matrix after PLS; *VIP*, Variable Importance; **Pharmacokinetic parameters:** *CL,* Body Clearance; CL_f, Fractal clearance; V_{ap}, Apparent volume of drug distribution; v_f, Fractal volume of drug distribution; **Molecular descriptors:** *fi,* Fraction ionized; *HAC,* Number of hydrogen bond acceptors; *HDO,* Number of hydrogen bond donors; *logD,* Apparent partition coefficient at pH 7.4; *logP*, Partition coefficient; *MW,* Molecular weight; *nPSsol,* Solvent accessible non-polar surface area; *nPSVdW*, Van der Waals non-polar surface area; *polrz*, Molecular polarizability; *Pssol,* Solvent polar surface area; *PSVdW*, Van der Waals polar surface area; *refr*, Molecular refractivity; *Ssol*, Solvent accessible molecular surface area; *SVdW*, Van der Waals molecular surface area; *Vsol*, Solvent accessible molecular volume; *VVdW*, Van der Waals molecular volume.

0724-8741/02/1200-1827/0 © 2002 Plenum Publishing Corporation

(20). A number of drugs were excluded due to certain molecular characteristics that might lead to unexpected behavior and/or do not permit reliable calculations of the molecular descriptors used in this study. These drugs were: quaternary ammonium compounds (e.g. pancuronium, atracurium, etc), molecules with very complicated chemical structures (cyclosporine, vancomycin, aminoglycosides, amphotericin-B, tacrolimus, macrolides etc.), drugs that include metal atoms in their structure (cis-platin, carboplatin, auranofin, gold sodium thiomalate) or are metals themselves (lithium), and unstable compounds like nitroglycerin or isosorbide. Thus, the number of the remaining data for further analysis was equal to 272.

Recently, the physiologically sound concept of fractal volume of drug distribution, v_f, was developed (18). This parameter takes values smaller or equal to the body mass (expressed in volume units) of the species and corresponds to the part of the total volume of the species body in which the drug is distributed at equilibrium. Eq. (1) (18) was used to calculate the v_f values from the reported V_{ap} values (20):

$$v_f = V_{pl} + (v - V_{pl})\left(1 - \frac{V_{pl}}{V_{ap}}\right) \quad (1)$$

where v is the total volume of the species body (equivalent to the total mass assuming a uniform density 1g/mL), and V_{pl} is the plasma volume of the species. In our study, the typical human values for v and V_{pl} (i.e., 70 and 3 L), were used respectively. The clearance analogue of v_f, called for reasons of uniformity fractal clearance. CL_f, refers to the portion of v_f that is cleared per unit of time (19). CL_f estimates were derived from Eq. (2) (19) using the reported CL, V_{ap} values, whereas v_f values were derived from Eq. (1):

$$CL_f = \frac{v_f}{V_{ap}} CL \quad (2)$$

The rational for this transformation relies on the fact that the quotients CL/V_{ap} and CL_f/v_f should be equal to the elimination rate constant (19). Due to the non-linear relationship between v_f and V_{ap} (Eq.1), Eq. (2) also expresses a non-linear transformation of CL to CL_f.

Filtered data (272 drugs) were classified into two classes according to their volume of drug distribution value. Based on the physiologic meaning of v_f and the relationship between v_f and V_{ap} Eq. (1) (18), the cutoff point of 67 L was assigned. Thus, drugs of class I have V_{ap} values lower than 67 L and therefore the quotient v_f/V_{ap} is higher than unity (18). For drugs of class II, v_f lies in the range 67–70 L (i.e., $v_f/V_{ap} < 1$); V_{ap} and v_f have the same value when V_{ap} is equal to 67 L. Class I comprises 131 drugs with small V_{ap} values, whereas class II comprises 141 drugs with higher V_{ap} values. Consequently, class I comprises drugs whose V_{ap} values are dilated when expressed in terms of v_f, whereas class II contains drugs whose V_{ap} values are shrinked when transformed to their v_f analogues.

A variety of physicochemical and molecular descriptors (data available upon request) were calculated using Pallas 2.0 (Compudrug Chemistry Ltd.) and Hyperchem v.5.0/ ChemPlus v.1.6 (Hypercube Inc.). The calculated descriptors express PK relevant fundamental properties including lipophilicity, ionization, molecular size and hydrogen bonding capacity.

Intrinsic lipophilicity was expressed by *logP* of the neutral species and *apparent lipophilicity* by *logD* at pH 7.4. Both parameters were calculated using the PrologP and PrologD modules of Pallas 2.0 upon application of two algorithms: *CDR* based on modified Rekker's fragmental procedure (25) and *ATOMIC5* (logPG-C) based on modified Ghose–Crippen atomic contribution system (26). Moreover the ChemPlus module implemented in Hyperchem v.5.0 was used for *logP* estimation according to the original Ghose–Crippen systems (logPG) (27). The mean *logP* and *logD* values derived from the different calculation procedures are expressed as *meanLP* and *meanLD*, respectively.

Dissociation constants were estimated using the pKalc module of Pallas 2.0 and expressed as acidic and basic pK_a. Several compounds had more than one acidic or basic center. In this case, only the pK_a for the most potent acidic and/or basic group was considered. Dissociation constants were used to categorize the drugs in term of acidic, basic or neutral function and to calculate the fraction ionized (*fi*) in pH 7.4 (in case of basic compounds).

Molecular size was expressed by molecular weight (*MW*) and a variety of descriptors: molar refractivity (*refr*), molecular polarizability (*polrz*), solvent accessible surface area (*Ssol*) or volume (*Vsol*), Van der Waals surface area (*SVdW*) or volume (*VVdW*), and molecular polar surface area based on solvent accessible surface area (*PSsol*) or Van der Waals surface area (*PSVdW*). For this purpose, all **O** and **N** atoms were considered as polar atoms. The corresponding non-polar surface areas, *nPSsol* and *nPSVdW*, were obtained by subtracting *PSsol* and *PSVdW* from *Ssol* and *SVdW*, respectively. All molecular size descriptors were calculated using the ChemPlus v.1.6 module implemented in Hyperchem v.5.0 after being subjected to 3-D optimization. The geometry of a given molecule was first optimized at the empirical level using an MM+ molecular mechanics force field, followed by unrestricted geometric optimization at the semi-empirical level using an SCF calculation with convergence limit set at 0.1 kcal/mol.

Hydrogen bonding capacity was expressed with two distinct descriptors; the number of hydrogen bond donors (*HDO*) and the number of hydrogen bond acceptors (*HAC*). *HDO* considers all O-H and N-H fragments. Hydrogen belonging to all kinds of acids and thiols were not counted (28). Likewise, *HAC* counts all oxygen and nitrogen atoms. Exceptions were the nitrogen in carbamides, sulfonamides, and the nitrogen atoms that are bound with three alkyl groups.

A multivariate data analysis of the disposition parameters described above (CL, V_{ap}, CL_f, v_f) was performed with SIMCA-P v.8.0 (Umetri AB, Umea Sweden). PCA was applied to the total set of literature data as well as to the two classes (class I, class II), separately. PCA is a multivariate projection method to extract and highlight the systematic variables in a data matrix **X**. Furthermore, PLS (projection to latent structures) was used to analyze each class of data separately. PLS is a regression extension of PCA applied to connect the information in the two blocks of variables **X** and **Y.** In our case, **X** comprises the descriptor matrix and **Y** the PK parameters. This relation is reflected in the *u-t* plot (see Abbreviations); the ideal behavior is a linearity between the *u* and *t* scores. The predictive ability of each model was evaluated using several statistical tools (29–31). First, cross-validation (*CV*) was applied, using the default values of SIMCA-P. The second validation tool was based on the ran-

domization of the responses. Scrambled **Y** data were the same with the original data set but were permuted to appear in a different order. Finally, each parent set of class I and class II was split into a training and a validation set. PLS models for each one of the classes were derived based only on the training sets, which then were used to predict the values of the validation set.

RESULTS AND DISCUSSION

PCA Models

A PCA was performed using the whole data set (314 drugs). All available descriptors (**X** variables) were used along with the four response variables (CL, V_{ap}, CL_f, v_f). The goal of this task was to determine strong outliers. Principal component analysis resulted in a model with two principal components (according to *CV*). The cumulative values of regression parameters (R^2 and Q^2) are presented in Table I. Data points lying outside the 95% confidence ellipse (Hotelling T^2) constitute strong outliers, Fig. 1. Due to their structural characteristics, these drugs and the compounds lying marginally in the accepted region were expected to behave differently. Indeed, these data were found to be almost identical with the data that had been *a priori* considered to be excluded from the analysis. Subsequently, the total data set of 314 drugs was split into 2 classes, according to the v_f/V_{ap} ratio as described in the "Methods" section. PCA models were built for each class separately. Both data sets were described by two principal components with R^2 and Q^2 values listed in Table I. It is also worthy to mention that the outliers derived from the separate PCA of the two classes coincide with those identified when PCA was applied to the aforementioned total data set. Hence, the rational for the exception for these drugs was anew justified and the remaining 272 observations comprised our data set for further PLS analysis.

PLS Models

Effort was given to develop a model for each PK parameter separately. No adequate PLS model for CL, V_{ap}, CL_f could be obtained with the used parameters. The u_1 *vs.* t_1 plots, which show the PLS inner relation between responses

Table I. Correlation Coefficients (R^2, Q^2) and Number of Significant Components (A) for Each Model

Model	Number of data	A	R^2	Q^2
PCA models				
Total data set	314	2	0.706	0.654
Class I	131	2	0.883	0.841
Class II	141	2	0.849	0.796
PLS models for v_f				
Subcluster I_a	29[a]/30[b]	1	0.627	0.618
Subcluster I_b	101[a]/101[b]	1	0.548	0.530
Class II	132[a]/141[b]	1	0.545	0.537
Training sets				
Subcluster I_a	21	1	0.621	0.607
Subcluster I_b	87	1	0.585	0.579
Class II	111	1	0.547	0.533

[a] Number of used data.
[b] Number of available data.

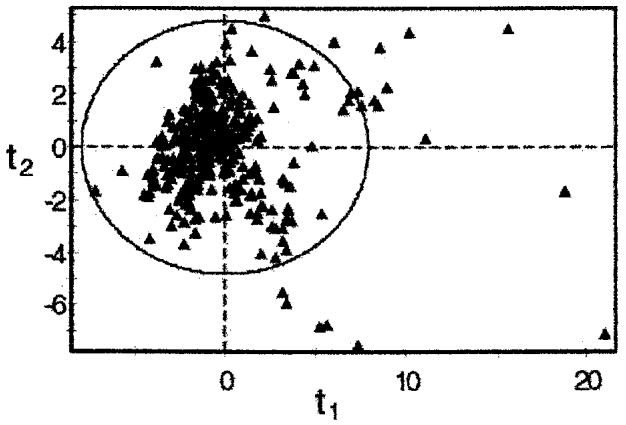

Fig. 1. The t_1 vs. t_2 score derived from PCA applied to the total data set (314 drugs).

and descriptors did not express any correlation or trend, either for the whole data set or for each one of the classes. To improve the statistics, a large portion of data (up to the half number of the total data) was excluded. The decision that drugs should be removed was based on visual observation of the u_1 *vs.* t_1 plots. In parallel, the descriptor matrix was reduced in terms of variable importance contribution (*VIP*) (30), as an effort to get better results. Despite of these alterations, the correlation coefficients were always relatively low. Using considerably reduced datasets, R^2 did not exceed 0.550, and Q^2 0.450.

On the contrary, adequate PLS models for each one of the two classes I and II were obtained when the parameter v_f was analyzed. The initial PLS analysis for class I resulted in non-satisfactory statistics. However, the inner relation shown in Fig. 2 indicates the presence of two potential subgroups. On the basis of the data trend, the encircled drugs of Fig. 2 exhibit lower values of v_f (reflected as u_1) than expected. This behavior was attributed to the effect of protein binding on the extent of drug distribution (32), because the encircled drugs of Fig. 2 exhibit higher protein binding than the remaining data. In fact, the mean value of the bound fraction, f_b, for the encircled data of Fig. 2 is 0.88, whereas for the remaining is

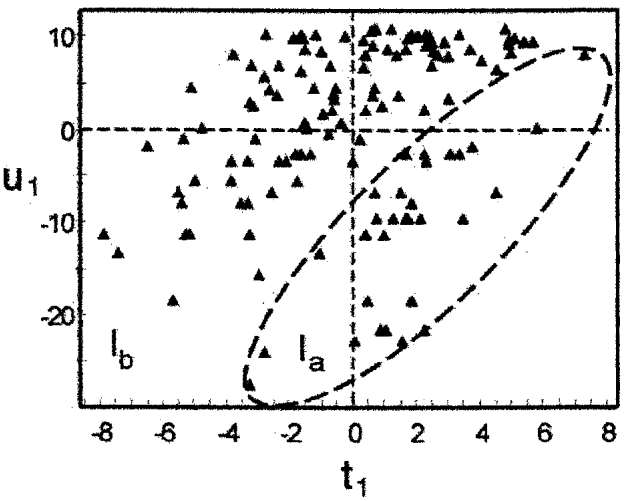

Fig. 2. The u_1 vs. t_1 plot showing the PLS relation for drugs of class I using v_f as response variable. See text for the encircled data.

0.56. Accordingly, two subclusters were defined: the 30 drugs within the encircled area formulated subcluster I_a, whereas the remaining (101) drugs were considered to belong to subcluster I_b. A 3-D representation of f_b vs. u_1 and t_1 (i.e., the two coordinates of Fig. 2) is shown in Fig. 3. This figure reveals that the domain where I_a drugs are lying (high t_1 and low u_1 values; dashed area on the u_1-t_1 plane), comprises drugs whose f_b values tend toward unity, whereas the remaining drugs belong to domain I_b.

Further PLS analysis of each subcluster I_a, I_b and class II was performed utilizing the *VIP* criterion for the selection of descriptors. One component models were derived for the segmented sets of data with R^2 and Q^2 values listed in Table I. Figure 4 A–C, shows the u_1, t_1 scatter plot for class I_a, I_b, and II, respectively. The regression coefficients of the descriptors for the three PLS models described above are shown in Fig. 5 A–C. In case of class I_a, one drug (diflunisal) proved to be outlier and was excluded from the analysis. In the PLS analysis of class II, 132 out of 141 drugs were included. The nine excluded outliers were: amiloride, cytarabine, finasteride, lidocaine, midazolam, nitrendipine, risperidone, trazodone, and triamterene. For the sake of completion, V_{ap} data were re-analyzed considering subgroups I_a and I_b separately. The results obtained with this parameter were again unsatisfactory.

Validation

After the establishment of QSPR models for v_f, the predictive ability of the models was tested. This task was implemented by using the statistical tools described in the "Methods" section.

Permutation tests were based on the recalculation of the models for randomly reordered response data. Figure 6 A–C shows the results for the three models after 50 permutation tests where R^2 and Q^2 estimates were plotted against the correlation coefficient ($R_{\mathbf{Y}}$) of the **Y** vector itself (i.e., this axis characterizes the degree of correlation between permuted and original **Y** data). The intercepts of both R^2, Q^2 regression lines were below zero indicating robustness of the models. Slightly worse results were obtained for class I_a model, Fig. 6A.

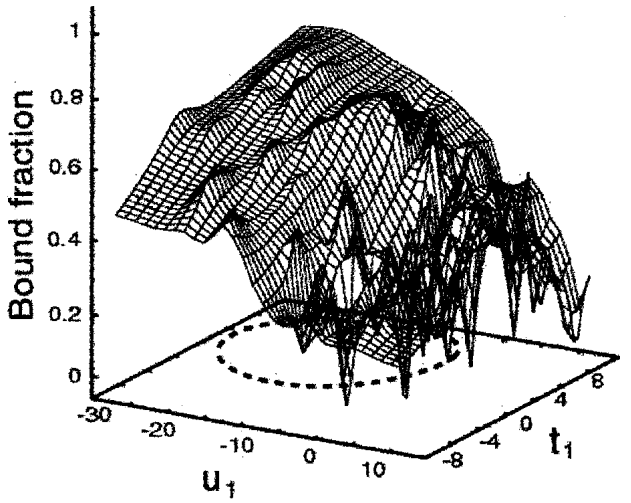

Fig. 3. The 3-D relationship for the bound fraction (f_b) of class I drugs with the u_1 and t_1 values derived from the PLS analysis shown in Fig. 2. Dashed ellipse on the u_1-t_1 plane represents the projection of the space that is occupied from I_a drugs.

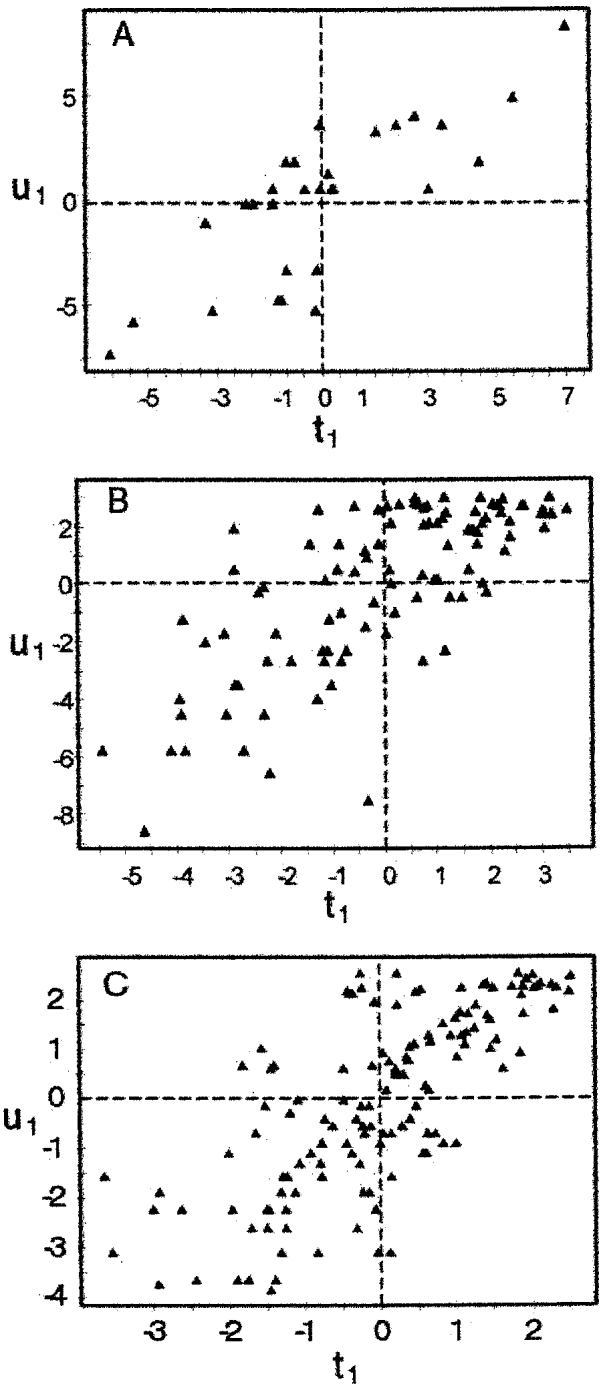

Fig. 4. The u_1 vs. t_1 plot showing the PLS relation for: subcluster I_a (A), subcluster I_b (B), and class II (C).

The validation—training sets were formulated using a random generator program developed in Mathematica 4.0 (Wolfram Research, Inc.). Approximately, 20% of the drugs belonging to the three data sets (subclusters I_a and I_b and class II) were selected for the validation sets. The newly derived PLS models for the training sets of each class were almost identical with those obtained from the whole data sets, because both the correlation coefficients and the contribution of descriptors expressed the same behavior. The observed vs.

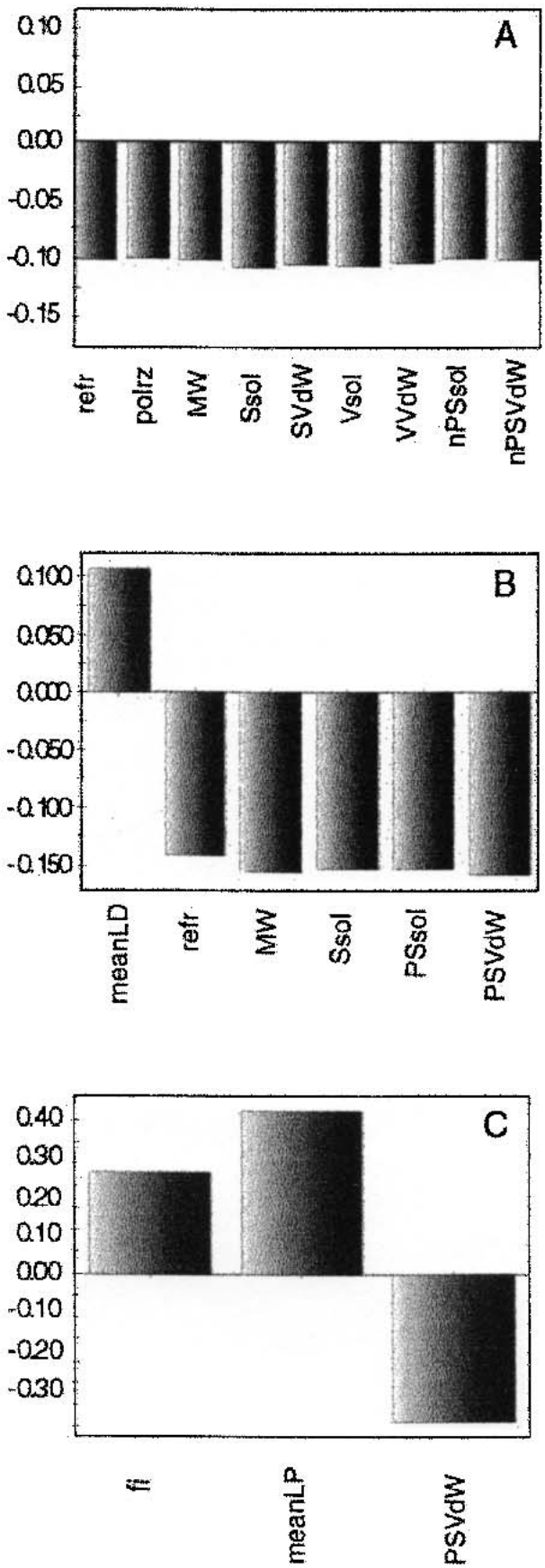

Fig. 5. Regression coefficients for the three models describing v_f response for drugs of: subcluster I_a (A), subcluster I_b (B), and class II (C).

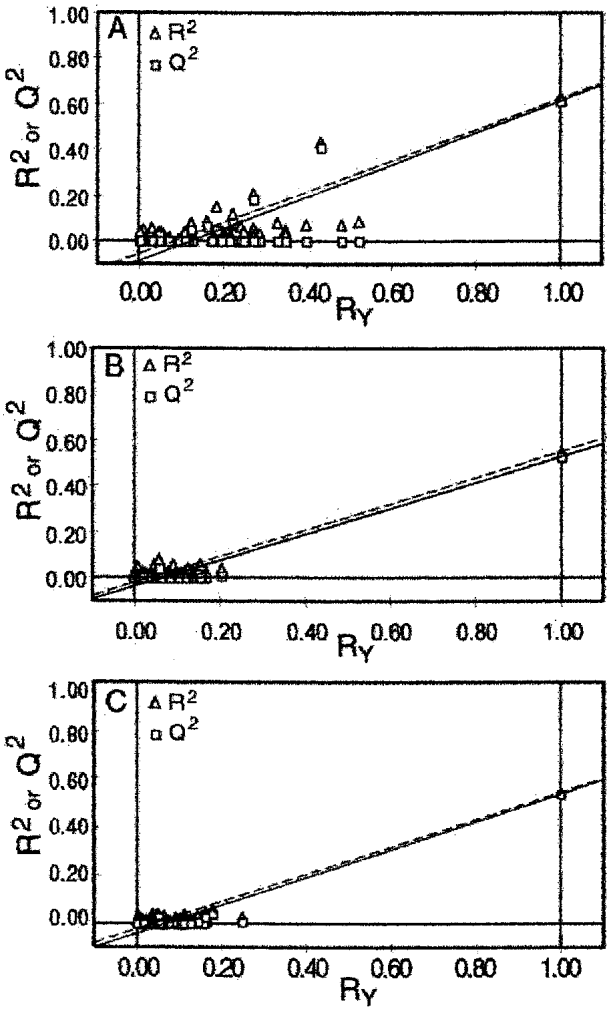

Fig. 6. Validation plot (based on 50 randomization cycles) for the three models describing v_f responses for drugs of: subcluster I_a (A), subcluster I_b (B), and class II (C). R_Y refers to the correlation coefficient of the **Y** vector itself.

predicted v_f values for each set of drugs are shown in Fig. 7 A–C, whereas the correlation coefficient values for the new models derived are presented in Table I. The RMSEP values shown in Fig.7 A–C were higher for class I_a and I_b than class II. However, this observation originates from the different range of the data values (i.e., 3 – 67 L for classes I_a, I_b, and 67–70 L for class II). This successful validation (Fig. 7) in conjunction with the permutations results (Fig. 6) allows one to infer that the developed models are reliable, especially for subcluster I_b and class II that include a large number (101 and 132, respectively) of structurally diverse drugs. In case of class I_a, we cannot be confident at the same degree due to the small amount of data (29 drugs).

Molecular Descriptors—Disposition Parameters: Overview

The inability to approximate any correlation between V_{ap}, CL, CL_f and a large variety of molecular descriptors lead to useful conclusions. Overall, the three parameters globally attempt to express drug distribution (V_{ap}) and elimination (CL, CL_f) but according to our results fail to reflect the physicochemical properties of drugs.

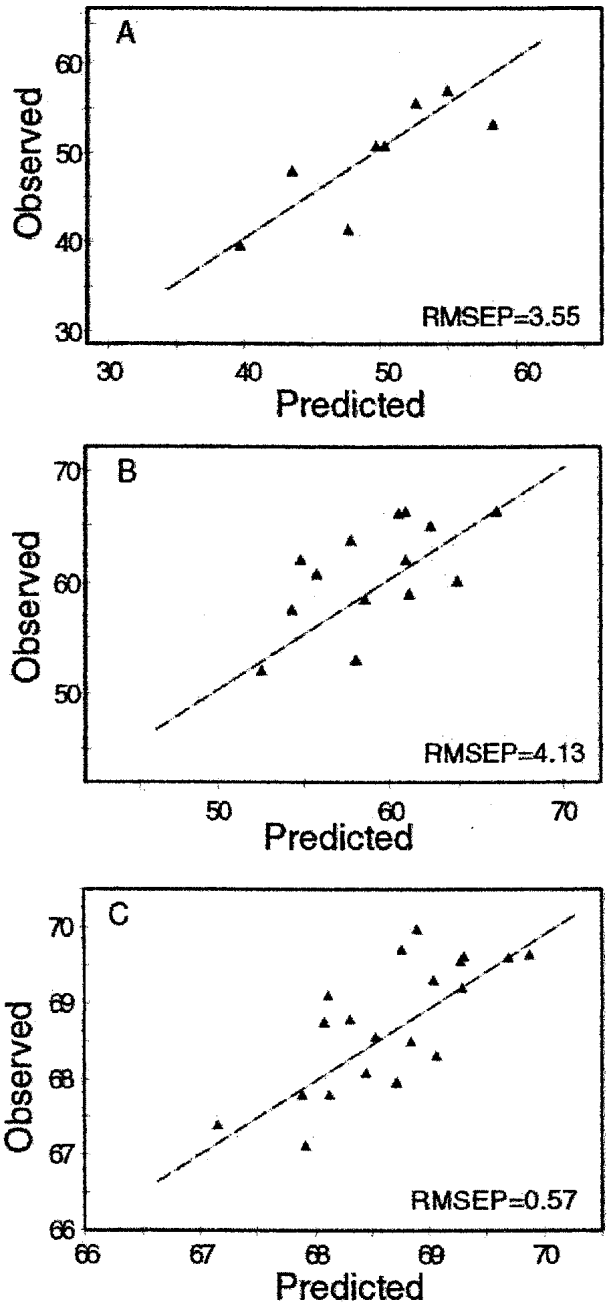

Fig. 7. Predicted vs. observed values of v_f for the three models describing drugs of: subcluster I_a (A), subcluster I_b (B), and class II (C). The dashed line indicates complete concordance. The values correspond to root mean square error prediction (RMSEP).

For V_{ap}, the fictitious numerical values reported in literature are the most plausible interpretation for this failure. It seems likely that the V_{ap} values provide only a qualitative measure for the distribution of drug in the body but fail to quantify it. This drawback originates from the heterogeneity of the human body in conjunction with the experimental methods used for the estimation of V_{ap}. Unavoidably, V_{ap} estimates are exclusively derived from drug measurements in plasma that is a homogeneous space but a tiny portion of the heterogeneous body.

In the same vein, a number of physiologically based causes can be quoted for the failure in establishing correlation between CL, CL_f and the molecular descriptors. These parameters express the volume cleared per unit of time and therefore are highly affected by the way we conceive the volume of drug distribution (fractal (18,19) or classic). Besides, CL and CL_f are composite and in essence hybrid parameters because different physicochemical factors govern renal and hepatic processes. In addition, the time dependent or stochastic character of the clearance terms cannot be ruled out if one takes into account the diffusion of drugs in the heterogeneous spaces of the human body and the complexity of elimination processes. Relevant remarks have been reported in literature sporadically (33–38).

The transformation of V_{ap} values to v_f using Eq. (1) seems to be the underlying cause for the valid models found for v_f. These findings allow a global consideration of the physicochemical properties that govern the distribution of drugs in the human body. To interpret the results for v_f in a comparative manner, the frequency distribution of v_f values for the three classes is presented in Fig.8. The mean value of v_f follows the ranking: $I_a < I_b < II$, whereas the composition of classes in terms of ionic centers indicates that the acid/base ratio decreases dramatically as we move from left to right, Fig. 8. Lipophilicity and apparent lipophilicity are moderate in class I_a, lower in class I_b, and higher in class II. Lipophilicity, either intrinsic or apparent, seems not to play a dominant role in v_f for class I_a (Fig. 5A). Molecular size descriptors contribute in a negative way to v_f, which constitutes a reasonable finding. Moving from class I_a to class I_b (Fig. 5B) the negative contribution of bulk descriptors is reflected in molecular refractivity and molecular weight. Molecular polar

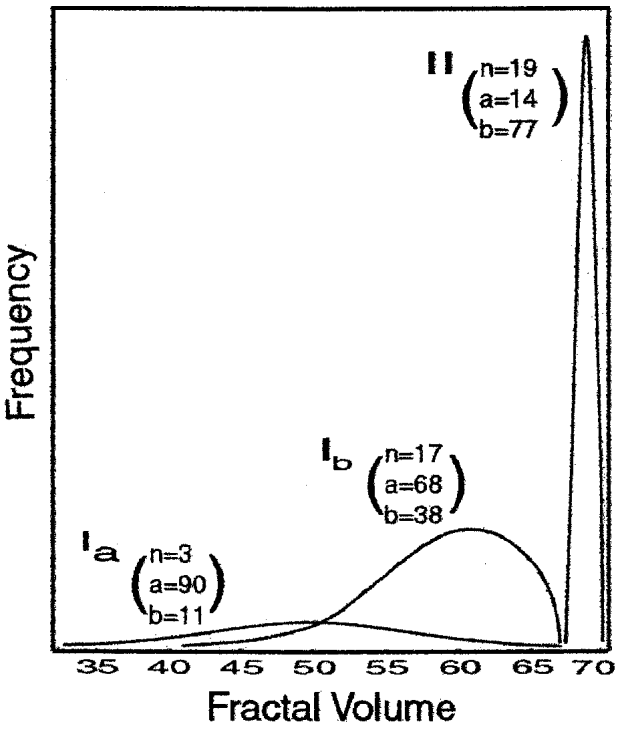

Fig. 8. Frequency distribution of the v_f values for class I_a, I_b, and II. The relative size of the areas under the curves corresponds to the number of drugs in each class: 29 (I_a), 101 (I_b) and 132 (II). The (%) ionic center composition of the compounds is presented next to the name of each class. Key (%): n = neutral, a = acidic, and b = basic compounds.

surface area is an additional negative factor, while apparent lipophilicity expressed as *logD* has a positive effect on v_f. Class II comprises drugs with large v_f values and includes mainly basic, lipophilic compounds, Fig. 8. Molecular polar surface area contributes in a negative way to v_f, whereas lipophilicity has a positive impact (Fig. 5C). In this model, the fraction ionized (*fi*) concerning the basic function seems a dominant variable with a positive sign, indicating that next to lipophilicity protonation is also important for the movement of basic drugs to peripheral tissues.

CONCLUSION

Due to their composite character, the parameters V_{ap}, CL, CL_f do not exhibit any correlation with the molecular descriptors. Two drug classes (I, II) were formulated on the basis of PLS models derived for v_f. Class I was further separated in two subclusters I_a and I_b. High protein binding was found as the dominant factor, whereas molecular size contributes in a negative way to v_f for class I_a drugs. For class I_b, v_f has a trend to increase with the increase of apparent lipophilicity whereas molecular refractivity, molecular weight, solvent surface area and polar surface area enter with a negative sign. For class II, v_f increases with the increase of lipophilicity and basicity of compounds whereas polar surface area has a negative contribution.

Overall, this study elucidates the relationships between the molecular descriptors and v_f. Because the correlations found for v_f were based on a great number of structurally unrelated drugs, one can anticipate the development of QSPR models when specific drug categories will be used. These models will certainly be practically useful for predictive purposes.

ACKNOWLEDGMENTS

This work was supported by the General Secretariat of Research and Technology of Greece (PENED 2001).

REFERENCES

1. M. O. Fouchécourt, M. Béliveau, and K. Krishnan. Quantitative structure-pharmacokinetic relationship modeling. *Sci. Tot. Environm.* **274**:125–135 (2001).
2. D. Alker, S. F. Cambell, P. E. Cross, R. A. Burges, A. J. Carter, and D. G. Gardiner. Long-acting dihydropyridine calcium antagonists. Synthesis and structure-activity relationships for a series of basic and nonbasic derivatives of 2-[(2-aminoethoxy)-methyl]-1,4-dihydropyridine calcium antagonists. *J. Med. Chem.* **33**:586–591 (1990).
3. A. Haj–Yehia and M. Bialer. Structure-pharmacokinetic relationships in a series of valpromide derivatives with antiepileptic activity. *Pharm. Res.* **6**:683–689 (1989).
4. E. Toma. Structure-activity relationship of quinolones. *Clin. Invest. Med.* **12**:7–9 (1989).
5. G. V. Betageri and J. A. Rogers. Correlation of partitioning of nitroimidazoles in the n-octanol/saline and liposome systems with pharmacokinetic parameters and quantitative structure-activity relationships (QSAR). *Pharm. Res.* **6**:399–403 (1989).
6. C. T. Gombar, R. M. Demarinis, M. Wise, and B. A. Mico. Pharmacokinetics of a series of 6-chloro-2,3,4,5-tetrahydro-3-substituted-1H-3-benzazepines in rats. Determination of quantitative structure-pharmacokinetic relationships. *Drug Metab. Dispos.* **16**:367–372 (1988).
7. T. Esaki. Quantitative drug design studies. Quantitative structure-activity relationships of ionizable substances: antibacterial activities of phenols. *Chem. Pharm. Bull.* **35**:3105–3111 (1987).
8. U. Ganzinger. Distribution properties of cephalosporin in man: pharmacokinetic and experimental approaches. *Int. J. Clin. Pharmacol. Ther. Toxicol.* **25**:262–278 (1987).
9. F. Gaspari and M. Bonati. Correlation between n-octanol/water partition coefficient and liquid chromatographic retention for caffeine and its metabolites, and some structure-pharmacokinetic considerations. *J. Pharm. Pharmacol.* **39**:252–260 (1987).
10. R. S. Markin, W. J. Murray, and H. Boxenbaum. Quantitative structure-activity study on human pharmacokinetic parameters of benzodiazepines using the graph theoretical approach. *Pharm. Res.* **5**:201–208 (1988).
11. E. Okezaki, T. Terasaki, M. Nakamura, O. Negata, H. Kato, and A. Tsuji. Structure-tissue distribution relationship based on physiological pharmacokinetics for NY-198, a new antimicrobial agent, and the related pyridonecarboxylic acids. *Drug Metab. Dispos.* **16**:865–874 (1988).
12. J. V. Gobburu and W. H. Shelver. Quantitative structure-pharmacokinetic relationships (QSPR) of beta blockers derived using neural networks. *J. Pharm. Sci.* **84**:862–865 (1995).
13. R. A. Herman and P. Veng-Pedersen. Quantitative structure-pharmacokinetic relationship for systemic drug. Distribution kinetics not confined to a congeneric series. *J. Pharm. Sci.* **83**:423–428 (1994).
14. W. J. Egan, K. M. Merz, and J. J. Baldwin. Prediction of drug absorption using multivariate statistics. *J. Med. Chem.* **43**:3867–3877 (2000).
15. M. D. Wessel, P. C. Jurs, J. W. Tolan, and S. M. Muskal. Prediction of human intestinal absorption of drug compounds from molecular structure. *J. Chem. Inf. Comput. Sci.* **38**:726–735 (1998).
16. F. Yoshida and J. G. Topliss. QSAR model for drug human oral bioavailability. *J. Med. Chem.* **43**:2575–2585 (2000).
17. X. C. Fu and W. Q. Liang. A simple model for the prediction of corneal permeability. *Int. J. Pharm.* **232**:1193–1197 (2002).
18. V. Karalis, L. Claret, A. Iliadis, and P. Macheras. Fractal volume of drug distribution: it scales proportionally to body mass. *Pharm. Res.* **18**:1056–1060 (2001).
19. V. Karalis and P. Macheras. Drug disposition viewed in terms of the fractal volume of distribution. *Pharm. Res.* **19**:697–704 (2002).
20. J. G. Hardman, L. E. Limbird, P. B. Molinoff, R. W. Ruddon, and A. G. Gilman, *Goodman and Gilman's The pharmacological basis of therapeutics*, 9th ed, The McGraw–Hill companies, New York, 1996.
21. R. Franke and A. Gruska. Principal component and factor analysis. In H. van de Waterbeemd (ed), *Chemometric methods in molecular design*, VCH, Weinheim, 1995, pp.113–158.
22. L. Eriksson and E. Johansson. Multivariate design and modeling in QSAR. *Chemom. Intell. Lab. Syst.* **34**:1–19 (1996).
23. L. Eriksson, J. L. Hermens, E. Johansson, H. J. Verhaar, and S. Wold. Multivariate analysis of aquatic toxicity data with PLS. *Aquatic Sciences* **57**:217–241 (1995).
24. S. Wold. PLS for multivariate linear modeling. In H. van de Waterbeemd (ed) *Chemometric methods in molecular design*, VCH, Weinheim, 1995 pp.195–218.
25. R. F. Rekker and H. M. de Kort. The hydrophobic fragmental constant: an extension to a 1000 data point set. *Eur. J. Med. Chem.* **14**:479–488 (1979).
26. A. K. Ghose and G. M. Grippen. Atomic physicochemical parameters for three-dimensional structure-directed quantitative structure-activity relationships. I.Partition coefficients as a measure of hydrophbicity. *J. Comput. Chem.* **7**:565–577 (1986).
27. V. N. Viswanadhan, A. K. Ghose, G. R. Revankar, and R. K. Robins. Atomic physicochemical parameters for three-dimensional structure-directed quantitative structure-activity relationships. Additional parameters for hydrophobic and dispersive interactions and their application. *J. Chem. Inf. Comput. Sci.* **29**:163–172 (1989).
28. T. I. Oprea. Property distribution of drug-related chemical databases. *J. Comput. Aided Mol. Des.* **14**:251–264 (2000).
29. S. Wold and L. Eriksson. Validation tools. In H. van de Waterbeemd, (ed) *Chemometric methods in molecular design*, VCH, Weinheim, 1995 pp.309–318.
30. T. I. Oprea and J. Gottfries. Toward minimalistic modeling of oral drug absorption. *J. Mol. Graphics Mod.* **17**:261–274 (1999).
31. S. Winiwarter, N. M. Bonham, F. Ax, A. Hallberg, H. Lennernas, and A. Karlén. Correlation of human jejunal permeability (in

vivo) of drugs with experimentally and theoretically derived parameters. A multivariate data analysis. *J. Med. Chem.* **41**:4939–4949 (1998).
32. S. Qie. Drug distribution and binding. *J. Clin. Pharmacol.* **26**:583–586 (1996).
33. M. Wise. Negative power functions of time in pharmacokinetics and their implications. *J. Pharmacokinet. Biopharm.* **13**:309–346 (1985).
34. J. B. Bassingthwaighte and D. A. Beard. Fractal 15O-labeled water washout from the heart. *Circ. Res.* **77**:1212–1221 (1995).
35. P. Macheras. A fractal approach to heterogeneous drug distribution: Calcium pharmacokinetics. *Pharm. Res.* **13**:663–670 (1996).
36. K. H. Norwich. Noncompartmental models of whole-body clearance of tracers: a review. *Ann. Biomed. Eng.* **25**:421–439 (1997).
37. M. Weiss. The anomalous pharmacokinetics of amiodarone explained by nonexponential tissue trapping. *J. Pharmacokinet. Biopharm.* **27**:383–396 (1999).
38. L. Claret, A. Illiadis, and P. Macheras. A stochastic model describes the heterogeneous pharmacokinetics of cyclosporin. *J. Pharmacokinet. Pharmacodyn.* **28**:445–463 (2001).